A Compact Rejection Filter based on Spoof Surface Plasmon Polartions and Folded Split-Ring Resonators with Controllable Rejection Bandwidth

Luping Li, Peng Chen, Pengfei Zhu, and Kai Yang

School of Aeronautics and Astronautics
University of Electronic Science and Technology of China, Chengdu, 611731, P. R. China
lplees@outlook.com, chenp@uestc.edu.cn, uestc_zpf@163.com, kyang@uestc.edu.cn

Abstract **—** A novel rejection filter composed of the single comb-shaped spoof surface plasmon polariton (SSPP) and the folded split-ring resonators (FSRR) is proposed in this letter. By embedding the FSRRs into grooves of the low-pass SSPP filter, the compact rejection filter with the same size as the low-pass filter is consequently realized. Compared with traditional ones, the proposed filter provides simpler structure, more compact size, lower insertion loss, higher frequency and controllable rejection bandwidth. The dispersion interprets the transmission modes of the rejection SSPP unit. And the approaches of controlling the rejection band prove the fine controllability in the filter. The fabricated filter has a size of $3.23\lambda_g\times0.24\lambda_g$, a central rejection frequency of 18.43 GHz, a fractional rejection bandwidth of 7.8%, maximum rejection depth of 42 dB, and an average passband insertion loss of 2.5 dB. The simulated rejection bandwidth controllable range is 4.0%~6.8%. Improved performances confirm the advantages of the proposed filter.

Index Terms **—** Compact rejection filter, controllable rejection bandwidth, folded split-ring resonator, spoof surface plasmon polariton.

I. INTRODUCTION

The surface plasmon polariton (SPP) is a kind of surface wave transmitting on the interface of substrate and dielectric in the infrared and optical band [1]. Owing to its ability to constrain the field to the subwavelength range from the interface, it has been applied to achieve a variety of optical devices. The SSPP is a manmade periodical array to imitate the subwavelength confine ability of the SPP in lower frequency bands and it has been applied into various microwave devices [2]-[4]. Due to its different design methods and ultra-wide passband characteristic than common filters, the SSPP filters are popular among microwave engineering [5]-[6].

The rejection filters loading rejection bands on passbands to reject unwanted signals in the passbands are indispensable devices for today's wideband communication systems. Since the SSPP just performs the wide passband frequency characteristic, it was attempted to achieve a rejection filter when the planar SSPP was first proposed [7]. Only one year later, Ref. [8] introduced some resonators to the side or back of the low-pass SSPP transmission line, where a rejection band was generated on the low-pass band and a rejection filter was realized. Reference [9] also achieved a similar rejection filter by etching resonators on the low-pass SSPP transmission line, where width of the SSPP transmission line was reduced. However, because the signal feeds of both filters are implemented through the coplanar waveguide, the filters still take wide areas. Reference [10] embeds the resonators into grooves of the SSPP transmission line and the signal feeding was achieved by the microstrip, where a more compact filter with much reduced width was presented. The dispersion of the rejection SSPP unit was also illustrated in Ref. [10], explaining the transmission modes of the rejection filter. However, the resonators in the mentioned filters all are double-ring ones, whose structures are relative complex and they are worth simplifying. In addition, none of these filters consider the control of the rejection bandwidth through the structural parameters.

This letter replaces the double-ring resonators of Ref. [10] with single-ring ones to achieve a simpler rejection filter with controllable rejection bandwidth. The dispersion of the rejection SSPP unit is also analyzed to illustrates the transmission modes of the rejection filter. Moreover, approaches of controlling the rejection frequency, the rejection depth, the rejection bandwidth and the filter's cutoff frequency through structural parameters all are detailed. The fabricated filter is also compared with traditional ones, which proves that the proposed one provides more compact filter size, higher rejection frequency, smaller insertion loss and controllable rejection bandwidth.

II. DISPERSION ANALYSIS

Schematic of the novel SSPPs unit is presented in Fig. 1 (a) and its structural parameters are listed in Table 1. The proposed SSPP unit embeds a folded split-ring resonator (FSRR) into groove of the single comb-shaped (SCS) SSPP unit. The SCS unit is a representative planar

Submitted On: September 15, 2018
Accepted On: May 12, 2019

SSPP unit and its fundamental dispersion mode is a low-pass one [7]. The schematic is designed on the substrate RT/duroid 5880 whose permittivity and thickness are 2.2 and 0.508 mm, respectively.

Dispersion of the SSPP unit is simulated in CST Microwave Studio and corresponding results are displayed in Fig. 1 (b). In the figure, the *Light Line* is the dispersion of the light transmitting in the vacuum. *Mode 0* and *Mode 1* are transmitting modes of the proposed SSPP unit. The yellow and blue regions are passbands of the SSPP unit and the gray one is a rejection band. Consequently, dispersion of the SSPP unit has a frequency characteristic of pass-reject-pass and the introduction of the FSRR inserts a rejection band on the passband of the SCS unit. Passbands of mode 0 and 1 are DC~17.86 GHz and 18.67~27.72 GHz, respectively. Accordingly, central frequency and bandwidth of the rejection band are 18.27 GHz and 0.81 GHz, respectively.

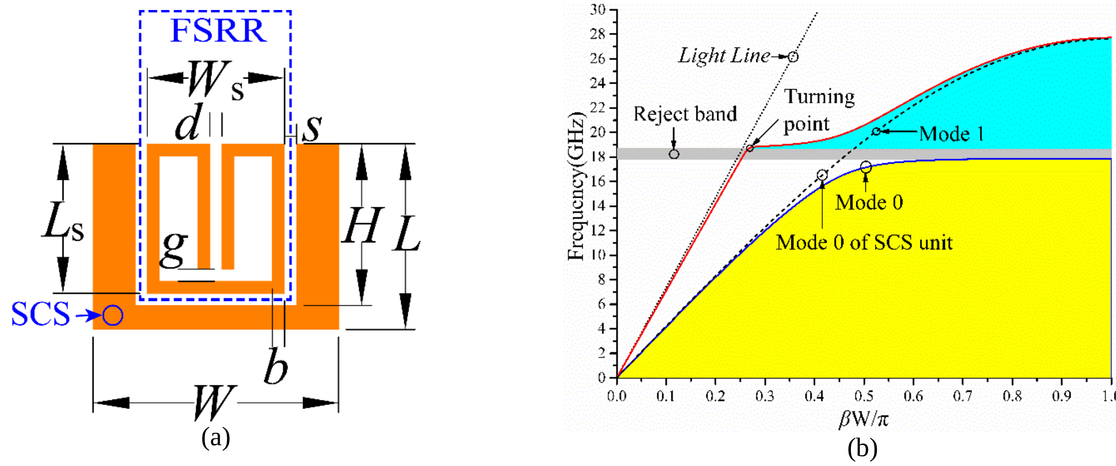

Fig. 1. Schematic and dispersion of the proposed SSPP unit: (a) the unit schematic and (b) the simulation dispersion.

Fig. 2. Schematic of the proposed rejection filter.

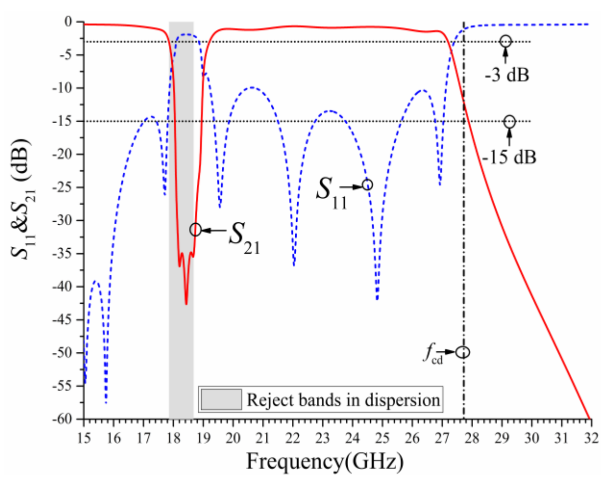

Fig. 3. Simulated S parameters of the proposed filter.

Table 1: Structural parameters of Fig. 1 (a)

Name	*L*	*W*	*Ls*	*Ws*
Value	1.54	2.04	1.24	1.14
Name	*H*	*d*	*s*	*g*
Value	1.34	0.1	0.1	0.1

III. FILTER SIMULATION

Due to the reject-pass-reject characteristic of the proposed SSPP unit, it is applied to achieve the proposed rejection filter in Fig. 2, where the SSPP part contains five periodical SSPP units and it determines the filter's frequency characteristics. The mode conversion parts transform the transmission modes of the microstrip and the SSPP bidirectionally and they are beneficial to the filter's performance. The microstrip is used for connecting with other microwave devices, width of which matches with 50 Ω characteristic impedance and it is 1.54 mm.

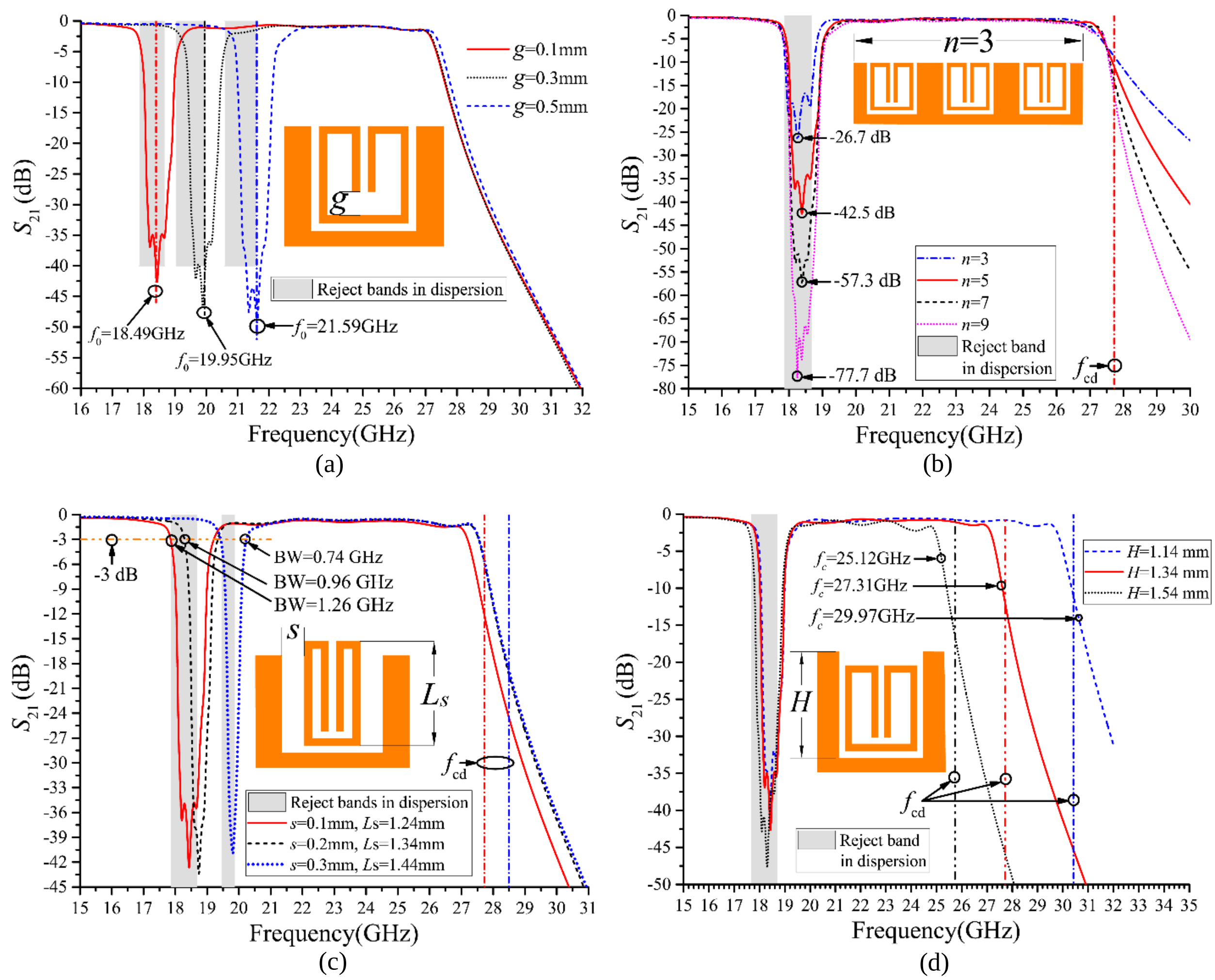

Fig. 4. Influence of the SSPP units on the frequency characteristics of the filter. (a) The influence of the FSRR length on the central rejection frequency; (b) the influence of the SSPP unit number on the rejection depth; (c) the influence of the structural parameter on the rejection bandwidth; (d) the influence of the groove depth on the filter's cutoff frequency.

The filter is simulated in CST Microwave Studio and simulation S parameters are displayed in Fig. 3, where the filter behaves one rejection band and two passbands. Central frequency and -3dB rejection bandwidth of the rejection band are 18.49 GHz and 1.26 GHz (6.8%), respectively. The -20dB rejection bandwidth and the maximal rejection depth are 0.84 GHz and 40.1dB, respectively. Moreover, the filter's cutoff frequency is 27.31 GHz and the average insertion losses in the passbands are 0.29 dB and 0.78 dB, respectively. Therefore, the filter provides a wide and deep rejection band.

The gray band in Fig. 3 is the rejection band of the dispersion, and f_{cd} is the cutoff frequency of *Mode 1*. According to the figure, the cutoff frequencies of the dispersion are closed to which of the filter, and the rejection bands of the dispersion are also entirely contained by which of the filter. This shows that frequency characteristics of the dispersion agree with those of the filter and the dispersion indicates the transmission modes of the SSPP units.

IV. FREQUENCY CHARACTERISTICS CONTROLLABILITY

To meet more demands in engineering applications, the methods of controlling the filter's S parameters through the structural parameters are discussed in this section.

A. Control on the central rejection frequency

In the proposed filter, the central frequency of the rejection band depends on the total length of the FSRR.

Accordingly, changing the length of the FSRR can alter the central frequency. The simulation results of three rejection filters with different *g* are illustrated in Fig. 4 (a) where the central frequency of the rejection band is increased by about 1.5 GHz when *g* increases by 0.1 mm, meanwhile the rejection bandwidth and the filter's cutoff frequency are roughly unchanged. The simulation result demonstrates that changing length of the FSRR can effectively control the central rejection frequency and make few impacts on other performances of the filter.

B. Control on the rejection depth

The effect of SSPP unit number on the rejection depth is shown in Fig. 4 (b), where the rejection depth is increased by about 16 dB as the SSPP unit number *n* increases by 2, and the central rejection frequency is maintained. In addition, the roll-off factor of the filter's cut-off band is also increased with the increasing of the SSPP unit number. Notably, dispersion of the SSPP unit remains unchanged in the whole process. The results indicate that number of the SSPP units can control the rejection depth and the roll-off factor. Meanwhile does not make influences on the central frequency of the rejection band.

C. Control on the rejection bandwidth

The influence of structural parameters on the rejection band is shown in Fig. 4 (c) where diverse *s* and *Ls* are set in different filters. According to the figure, the rejection band is decreased 0.52 GHz (2.8%) when *s* and *Ls* are increased 0.2 mm simultaneously, and the central frequency also shifts 1.31 GHz. Notably, total length of the FSRR in not changed in the processing, but the shape of the FSRR has been changed from a short and wide one into a high and thin one. It can be seen that the shape variation leads to changes in the rejection bandwidth and the central frequency. Besides, since the impact on the central frequency can be compensated by adjusting the FSRR's length, the rejection bandwidth control approach can be applied in engineering applications.

D. Control on the cutoff frequency

Groove depth *H* in low-pass comb-shaped SSPP filters almost decides their cutoff frequencies and it is usually used to control the cutoff frequencies. This approach is also applicable in the proposed rejection filter. Simulated S_{21} of three rejection filters with different *H* are illustrated in Fig. 4 (d), where the cutoff frequency is reduced by about 2.6 GHz as the groove depth increases by 0.2 mm, meanwhile the rejection band is nearly not affected. Two conclusions can be drawn from the simulation result. Firstly, the groove depth can effectively control cutoff frequency of the rejection filter. Secondly, frequency characteristics of the rejection band and the cutoff band are mutually independent and they can be independently controlled.

In conclusion, the approaches of controlling the central frequency, the rejection depth, the rejection bandwidth and the cutoff frequency are detailed in this section. The illustrated simulation results prove the fine frequency characteristics controllabilities of the proposed rejection filter and these controllabilities can be combined to meet different demands in practical designs. The application range of the filter is broadened by these controllabilities, especially the controllable rejection bandwidth contributes more to the broadening.

V. FABRICATION AND MEASUREMENT

Fabricated filter and microstrip are displayed in Fig. 5, where the microstrip is used for evaluating the additional loss from the welding, the substrate and the connectors. The filter and microstrip are put in the aluminum box to be measured by the vector network analyzer. Size of the filter is 40.0 mm×3.0 mm ($3.57\lambda_g \times 0.29\lambda_g$), where λ_g is the guided wavelength of the central rejection frequency. Substrate and length of the microstrip are same as the filter, where the characteristic impedance and length are 50 Ω and 40.0 mm, respectively.

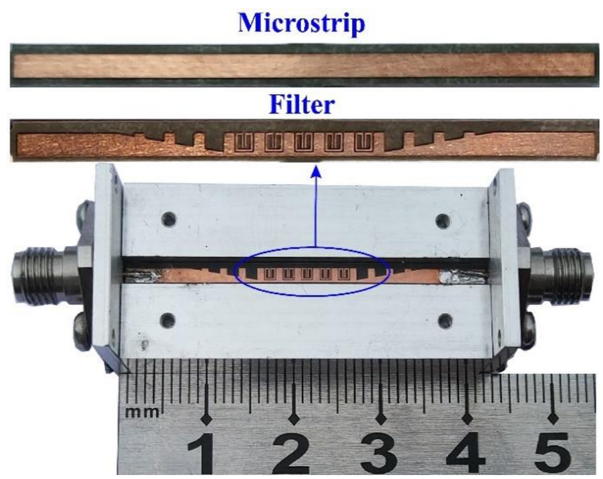

Fig. 5. Photograph of the fabricated filter and microstrip.

In the measurement, the microstrip is firstly measured and its S_{21} is normalized to 0 dB in the vector network analyzer before measuring the filter. Accordingly, measurement S_{21} of the filter has subtracted the loss of the microstrip. The measurement results are illustrated in Fig. 6, where the measurement S_{21} in Fig. 6 (b) is a result of taking away the measurement S_{21} in Fig. 6 (a). In the frequency band of 10-30 GHz of Fig. 6 (a), simulated and measured average insertion losses of the microstrip are 0.33 dB and 1.78 dB, respectively, hence the additional loss is about 1.45 dB.

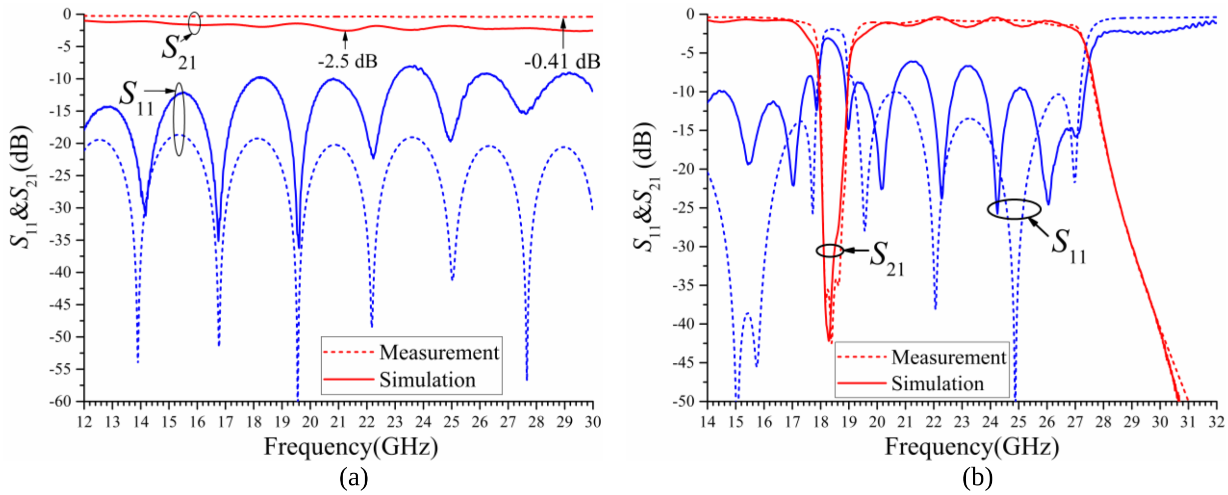

Fig. 6. Measurement S parameters of the fabricated filter and microstrip: (a) the microstrip and (b) the rejection filter.

Table 2: Comparison with SSPP rejection filters

Work	Size ($\lambda_g \times \lambda_g$)	f_0/GHz	*FBW* [1]/%	*IL*[2]/dB	Order	Depth	*RBC* [3]	Dispersion
[8]	5.64×1.40	6.75	1.9	4.6	8	-15	No	No
[8]	6.20×1.54	7.45	17.4	3.7	7	-42	No	No
[9]	13.4×3.18	8.15	5.8	5.5	5	-32	No	No
[9]	14.2×3.41	8.74	4.6	3.1	6	-33	No	No
[10]	5.85×0.15	14.47	14.7	4.3	5	-43	No	Yes
This work	3.23×0.24	18.43	7.8	2.5	5	-42	Yes	Yes

[1] *FBW* is the fractional rejection bandwidth;
[2] *IL* is the insertion loss of the passband;
[3] *RBC* is rejection bandwidth controllability.

As Fig. (b) demonstrates, central frequency and -3 dB bandwidth of the rejection band are 18.43 GHz and 1.45 GHz, respectively, thus the fractional rejection bandwidth is 7.9%. The -20dB rejection bandwidth is 0.84 GHz and the maximal rejection depth is 42.2 dB. The average insertion losses of two passbands are 0.58 dB and 1.02 dB, respectively. The filter's cutoff frequency is 27.32 GHz and the out-of-band rejection is greater than 60 dB. The measurement results agree well with the simulation, proving both the proposed filter and the design approach are available.

The comparison between traditional SSPP rejection filters and our filter is listed in Table 2, where the additional loss of our filter is taken into the total insertion loss. According to the table, the proposed filter provides more compact filter size, higher central frequency, middle rejection bandwidth and smaller insertion loss. In addition, the proposed filter gives the approach of controlling the rejection bandwidth for the first time. It can be concluded that the proposed filter has improved performances than traditional ones.

VI. CONCLUSION

By simplifying the structure of traditional SSPP units, a novel SSPP rejection filter with controllable rejection bandwidth is achieved in this letter. The dispersion is analyzed to explain the transmission mechanism of the rejection SSPP units. And the approaches of controlling the filter's S parameters through the structural parameters are also presented. The measured better performance than traditional filters proves that the proposed filter has an improvement from traditional ones.

ACKNOWLEDGMENT

This work was supported by the National Natural Science Foundation of China 61601088 and 61571093.

REFERENCES

[1] W. L. Barnes, A. Dereux, and T. W. Ebbesen, "Surface plasmon subwavelength optics," *Nature*, vol. 424, no. 6950, pp. 824-830, Aug. 2003.

[2] J. B. Pendry, "Mimicking surface plasmons with structured surfaces," *Science*, vol. 305, no. 5685, pp. 847-848, Aug. 2004.

[3] P.-S. Kildal, "Definition of artificially soft and hard surfaces for electromagnetic waves," *Electronics Letters*, vol. 24, no. 3, p. 168, 1988.

[4] P.-S. Kildal, "Artificially soft and hard surfaces in electromagnetics," *IEEE Transactions on Antennas*

and Propagation, vol. 38, no. 10, pp. 1537-1544, 1990.

[5] P. Chen, L. Li, K. Yang, and Q. Chen, "Hybrid spoof surface plasmon polariton and substrate integrated waveguide broadband bandpass filter with wide out-of-band rejection," *IEEE Microwave and Wireless Components Letters*, vol. 28, no. 11, pp. 984-986, Nov. 2018.

[6] J. Xu, et al., "Low-pass plasmonic filter and its miniaturization based on spoof surface plasmon polaritons," *Optics Communications*, vol. 372, pp. 155-159, Aug. 2016.

[7] X. Shen and T. Jun Cui, "Planar plasmonic metamaterial on a thin film with nearly zero thickness," *Applied Physics Letters*, vol. 102, no. 21, p. 211909, May 2013.

[8] B. C. Pan, Z. Liao, J. Zhao, and T. J. Cui, "Controlling rejections of spoof surface plasmon polaritons using metamaterial particles," *Optics Express*, vol. 22, no. 11, p. 13940, June 2014.

[9] Q. Zhang, H. C. Zhang, J. Y. Yin, B. C. Pan, and T. J. Cui, "A series of compact rejection filters based on the interaction between spoof SPPs and CSRRs," *Scientific Reports*, vol. 6, no. 1, p. 28256, Sep. 2016.

[10] S. Zhao, H. C. Zhang, J. Zhao, and W. X. Tang, "An ultra-compact rejection filter based on spoof surface plasmon polaritons," *Scientific Reports*, vol. 7, no. 1, p. 10576, Dec. 2017.

Luping Li received his Bachelor degree in Electronic Information Engineering from Chengdu University of Information Technology (CUIT) in 2016. Now he is studying his Master degree in University of Electronic Science and Technology of China (UESTC) since September 2016. His research interests are RF/microwave filters and metamaterials.

Peng Chen received Bachelor in Electronic Science and Technology and Ph.D. degree in Circuits and Systems from University of Electronic Science and Technology of China (UESTC) in 2009 and 2015, respectively, where he became a Lecturer in 2015. He was also a visiting scholar in Tohoku University, Sendai, Japan from November 2017 to November 2018. His main research interests are design and optimization RF and microwave devices and systems.

Pengfei Zhu received his Bachelor degree in Radio Wave Propagation and Antenna from University of Electronic Science and Technology of China (UESTC) in 2016, he is studying his Master degree at UESTC since September 2016. His research interests are RF/microwave circuits and systems.

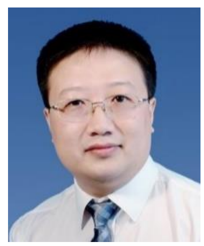

Kai Yang became an Associate Professor and a Professor of University of Electronic Science and Technology of China (UESTC) in 2001 and 2007, respectively. He became a Senior Member of Chinese Institution of Electronics in 2006. His research interests are RF/microwave circuits and systems, superconducting microwave components and circuit theory.